Published in final edited form as:

Curr Oncol Rep. 2015 December ; 17(12): 56. doi:10.1007/s11912-015-0480-y.

Novel Imaging of Prostate Cancer with MRI, MRI/US, and PET

Phillip J. Koo[1], **Jennifer J. Kwak**[1], **Sajal Pokharel**[2], and **Peter L. Choyke**[3]

[1]Division of Nuclear Medicine and Molecular Imaging, Department of Radiology, University of Colorado School of Medicine, Mail Stop L954, 12401 E. 17th Avenue, Room 1512, Aurora, CO 80045, USA

[2]Division of Abdominal Imaging, Department of Radiology, University of Colorado School of Medicine, Mail Stop L954, 12401 E. 17th Avenue, Room 1512, Aurora, CO 80045, USA

[3]Center for Cancer Research, National Cancer Institute, Building 10, Room B3B69F, Bethesda, MD 20892-1088, USA

Abstract

Imaging of prostate cancer presents many challenges to the imaging community. There has been much progress in this space in large part due to MRI and PET radiopharmaceuticals. Though MRI has been focused on the evaluation of local disease and PETon the detection of metastatic disease, these two areas do converge and will be complementary especially with the growth of new PET/MRI technologies. In this review article, we review novel MRI, MRI/US, and PET radiopharmaceuticals which will offer insight into the future direction of imaging in prostate cancer.

Keywords

Prostate cancer; MRI; MRI/US; Fusion; DWI; DKI; Hyperpolarized; PET; PET/CT; PSMA; FACBC; Acetate; Bombesin; GRP; FDHT

Phillip J. Koo phillip.koo@ucdenver.edu. Jennifer J. Kwak jennifer.kwak@ucdenver.edu. Sajal Pokharel sajal.pokharel@ucdenver.edu. Peter L. Choyke pchoyke@nih.gov.

Compliance with Ethics Guidelines

Conflict of Interest Phillip J. Koo has received compensation from Philips Healthcare, Bayer Healthcare, and Dendreon for service as a consultant.
Jennifer J. Kwak declares that she has no conflict of interest.
Sajal Pokharel declares that he has no conflict of interest.

Peter L. Choyke was issued a patent on an MRI-US fusion biopsy device known as UroNav. Dr. Choyke receives no royalties, however, and the National Cancer Institute receives licensing fees.

Human and Animal Rights and Informed Consent This article does not contain any studies with human or animal subjects performed by any of the authors.

Papers of particular interest, published recently, have been highlighted as:
• Of importance
•• Of major importance

Introduction

Current standard of care imaging for prostate cancer includes computed tomography (CT) and Tc-99m-based bone scanning [1•]. More advanced imaging technologies continue to be developed to improve accuracy at diagnosis, staging, and restaging, as well as monitor patients on active surveillance. These techniques will allow for more informed treatment decisions. The use of imaging will expand as its use as a biomarker for treatment response and prognosis continue to develop. For castrate-resistant prostate cancer (CRPC) patients, imaging will help optimize the sequencing of the multiple therapies now available. Imaging will also support a new era of theranostics which combines diagnostic tests with targeted therapies.

We review novel imaging techniques to image local and metastatic diseases. The discussion regarding the detection of local disease centers on the use of magnetic resonance imaging (MRI) and MRI/US. For metastatic disease, we focus on several non-FDA approved, promising PET radiopharmaceuticals which offer new methods to detect and monitor disease. Though these radiopharmaceuticals are currently only available in the research setting, they offer a glimpse into the future of prostate cancer imaging which will improve the care of our patients.

Prostate MRI

While the feasibility of MRI of the prostate gland was demonstrated in the 1980s, its utility in assessment of primary prostate cancer was established over the next decade with the advent of task-specific endorectal coils in the early 1990s which provided increased signal from the prostate gland and improvements in T2-weighted imaging [2, 3].

Subsequently, additional MRI sequences were developed, namely dynamic contrast-enhanced imaging (DCE), MR spectroscopy (MRS) (1990s), and diffusion weighted imaging (DWI) (2000s).

These functional sequences combined with traditional T2-weighted imaging are termed multi-parametric MRI (mpMRI). In current practice, most facilities performing mpMRI utilize DWI and DCE in addition to T2-weighted imaging. MRS is not widely included because it is resource intensive and the degree of added benefit may be limited [4]. Current consensus guidelines for prostate mpMRI from the European Society of Urologic Radiology, Admetech, and the American College of Radiology, which are known as PIRADS v2, emphasize DWI and DCE as the standard functional sequences and consider MRS optional [5, 6••]. mpMRI has been shown to be very accurate in the detection of clinically significant prostate cancer with a recent meta-analysis demonstrating a pooled specificity of 0.88, sensitivity of 0.74, and negative predictive value ranging from 0.65 to 0.94 for clinically significant prostate cancer [7•].

Non-targeted Systematic Biopsy

Prostate biopsies are typically performed in a systemic fashion without targeting a focal lesion. This standard of care method for diagnosing prostate cancer has consisted of trans-

rectal biopsies under ultrasound (US) guidance. The US is used to localize the global anatomy of the prostate gland and direct systematic biopsy of different segments of the gland rather than targeting focal lesions, which US has low sensitivity to detect [8]. This approach suffers from less than ideal sensitivity because random samples may miss lesions (especially anterior lesions) or may undersample the lesion, detecting only the low grade portion of a lesion [9]. Moreover, random biopsies tend to detect small low-grade cancers that are currently considered of no clinical significance but nonetheless require follow-up including repeat biopsy [10]. More recently, several methods of targeting focal lesions seen on MRI for biopsy have become available.

Direct MRI-guided Biopsy

Direct in-bore MRI-guided biopsy targets lesions with the patient in the MR scanner. While this technique may be the most accurate in targeting the lesion seen on MRI, it is logistically difficult [11]. Constraints include those related to performing a procedure in a strong magnetic field, which requires specialized materials. Direct MRI-guided biopsy also requires extended MRI scanner time, which is an expensive limited resource.

MRI-targeted-Ultrasound-guided Biopsy

Because of the constraints of direct MRI-guided biopsy, focus has shifted toward a combined biopsy approach, where US is the imaging modality used during biopsy but MRI data is incorporated to target lesions. This approach is accomplished in one of two main ways: cognitive registration and image fusion.

Cognitive Registration

Cognitive registration biopsy entails first performing mpMRI to detect prostate lesions. These lesions are then targeted for biopsy under US guidance, usually with the trans-rectal approach, using relative anatomy to target the expected location of the lesion. The “registration” in this technique is performed in the mind of the operator and is, thus, highly dependent on experience. The MRI lesion location in the prostate gland is viewed in relation to adjacent structures such as the urethra, the global gland anatomy, and perhaps other lesions such as BPH nodules. The main advantage of this technique is that it is relatively easy to implement and does not require additional hardware or software. The major drawback is that registration and targeting may not be as precise as other techniques owing to both the deformability of the prostate gland and the nonstandard and variable imaging planes of US as well as the skill of the operator. Nevertheless, in experienced hands, this technique has been shown to be relatively accurate and more efficient than non-targeted systematic biopsy [12, 13].

Image Fusion

Image fusion utilizes algorithms and hardware to overlay MRI data on real-time US images during US-guided biopsy. Most commonly, mpMRI is obtained, and the lesions and the whole prostate gland are then contoured. During the biopsy session, the prostate gland is again contoured on real-time US. The MRI and US data are then spatially registered and the contoured MRI lesions are overlayed on the real-time US images. As the operator adjusts the

US probe to view various parts of the prostate, the MRI data are also adjusted in real-time. Biopsy can then be directed to the location of the prostate where the MRI lesion is projected. Needle trajectory can be overlaid on the images to improve adequate sampling. Different vendors have developed variations of the technique, some utilizing software only and others requiring additional hardware. The fusion technique requires greater investment in software, sometimes hardware, MRI post-processing, as well as operator training. However, accuracy of lesion targeting appears to be improved relative to cognitive registration, with a recent study showing that cognitive registration detected less than half of the clinically significant cancers detected by fusion [14]. Furthermore, there is growing evidence which shows high accuracy, improved detection of clinically significant cancer, and decreased detection of clinically insignificant cancer with the fusion approach [15, 16, 17••, 18–20, 21••]. In a large prospective cohort study, Siddiqui et al. showed that targeted fusion biopsy diagnosed 30 % more high-risk cancers and 17 % fewer low-risk cancers versus standard TRUS biopsy [21••].

Novel Diffusion Techniques

DWI has become central to the success of mpMRI and is an active area of research. Traditional DWI assesses the Brownian (random) movement of water molecules in tissues. Malignant tissue tends to have more restricted water motion due to the large numbers of cell membranes and collagen stroma. The novel diffusion techniques attempt to refine the type of diffusion being probed and, thus, extract more specific information. The one technique which has entered clinical practice to a variable extent is “high *b*-value” DWI. The “*b*-value” is a measure of the strength of the magnetic gradient applied during image acquisition. DWI is typically performed at two or more lower *b*-values so the apparent diffusion coefficient (ADC) can be calculated. ADC is a more accurate representation of diffusion restriction than the primary diffusion signal. Traditionally, *b*-values ranged from 0 to 1000 s/mm^2. The high *b*-value approach is to use *b*-values of 1400 s/mm^2 or greater [6••, 22, 23]. High *b*-value DWI accentuates low-diffusion sites such as cancer compared to normal higher-diffusion tissue (normal background). The high *b*-value images demonstrate retained signal in tissues with more restricted diffusion (i.e. cancers) while the background normal tissue loses signal. Thus, lesions are more conspicuous. For example, Katahira et al. evaluated 201 cases with a histopathologic correlation and found that the sensitivity and specificity were improved when using a *b*-value of 2000 versus 1000 s/mm^2 (73 and 90 % versus 61 and 83 %, respectively) [23]. Figure 1 shows an example of a prostate gland lesion that was most conspicuous on high *b*-value DWI.

Advancement in DWI has also been seen with implementation of more detailed mathematical models of the diffusion signal. For example, diffusion kurtosis imaging (DKI) models the signal decay with increasing *b*-values using a polyexponential function rather than a monoexponential one [24]. DKI better correlates with the data especially at high *b*-values where the diffusion signal is more significantly affected by the intracellular environment [24]. DKI has been shown to improve accuracy in prostate cancer differentiation [25].

Improved Data Extraction

DKI is a form of image processing which extracts more useful information from the data already present. Textural analysis is another technique which assesses the variability of signal within a lesion to obtain quantitative parameters which can help differentiate malignant tissue [26]. A recent abstract by Rezaeilouyeh et al. describes an application of shearlet transformation, in effect, an enhanced edge detection algorithm, to obtain sensitivities of 92, 100, and 89 on T2W, DWI, and DCE images, respectively, in a small cohort [27]. Yet another approach is to use multiple computer-derived imaging parameters to define the characteristics of a tumor. Such methods are highly dependent on accurate histologic verification[28].

Hyperpolarized MRI

Clinical MRI has exclusively relied on the nuclear magnetic resonance (NMR) of the water proton, ^{1}H. Water protons are abundant in the body and, thus, provide high signal. The ubiquity of water is also a limiting factor, as the specificity of water signal is limited. Any element with a nuclear spin of one half can theoretically produce NMR signal. However, the concentrations of other potential elements of interest in the human body are too low for conventional imaging. Traditional MRS does probe compounds other than water but this has also traditionally been limited to the proton signal. Hyperpolarized MRI allows other elements to be imaged, particularly C13. This is accomplished by drastically skewing the quantum state of the nuclear spin of a specific element. Elements in this state can then produce enough signal to be measurable and useful although only for the short time they remain hyperpolarized.

In dynamic nuclear polarization, hyperpolarization is obtained by adding a free radical which couples with the substrate of interest and transfers some of its electron spin to the nucleus of interest. Then, the substrate is cooled to near absolute zero and irradiated with microwaves to induce the spins to mostly align in one direction. The substrate is then rapidly melted by dissolving it in solution, and after a quality control process, the compound is rapidly injected into the patient [29]. This method has been successfully accomplished in a limited number of humans using hyperpolarized ^{13}C-pyruvate which is converted to ^{13}C-lactate preferentially in cancer cells [30]. A wide variety of metabolites could be probed not only for tumor detection but also for characterization of cancer [29]. Potential drawbacks of the technique are its complexity, expense, the need for injection of an extraneous agent, and the rapid decay of hyperpolarization requiring rapid injection and imaging.

Pet Radiopharmaceuticals

Prostate-specific Membrane Antigen

Prostate-specific membrane antigen (PSMA) is a cell surface transmembrane glycoprotein with an intracellular component and a large extracellular component with enzymatic function also known as folate hydrolase or glutamate carboxypeptidase; however, the exact function of PSMA and its ligand are unknown [31–34]. PSMA expression is found in the normal prostate gland, but much higher expression is found in primary and metastatic prostate cancer [32, 35]. Despite its name, PSMA expression is also found outside the

prostate gland in the neovasculature of other solid tumors such as kidney, bladder, pancreas, and lung cancers, and low level expression is also demonstrated in the small intestines, proximal renal tubules, salivary glands, and brain [33, 36].

Currently, the only commercially available imaging agent for the detection of prostate cancer is a radiolabeled PSMA antibody, In-111 capromab pendetide (ProstaScint®), which was FDA-approved in 1996. ProstaScint® is a mouse monoclonal antibody that binds to the intracellular component of PSMA in apoptotic or necrotic tissue with limited sensitivity and specificity (~60 and ~70 %) including low detection of bone metastases [32, 35, 37, 38]. This suboptimal performance is attributed to the targeting of the intracellular domain of PSMA which limits detection to non-viable prostate cancer cells where the membrane is damaged. In addition to test performance issues, disadvantages of ProstaScint® include a long delay between injection and imaging, low lesion to background uptake, and human anti-mouse antibody reaction [39].

Several newer PSMA agents which target the external moiety of PSMA are currently being investigated for imaging and therapy. Due to better resolution of PET/CT imaging compared to SPECT/CT imaging, there is great interest in PET radiopharmaceuticals. New PSMA-based imaging agents include antibodies and small-molecule PSMA inhibitors [34].

J591 is a de-immunized monoclonal antibody that binds to the extracellular component of PSMA, and unlike ProstaScint®, can detect viable prostate cancer cells. It has been labeled with Zr-89 and Cu-64 for preclinical PET imaging and with Y-90 and Lu-177 for therapy [34]. A disadvantage with antibody-based agents is the delay between radiotracer administration and imaging to clear circulating, nonlocalizing antibodies for improved target to background ratio. For example, J591 tagged with Zr-89 for preclinical PET imaging studies required post injection delay of 5–7 days [40].

This challenge has been addressed with the introduction of small-molecule PSMA inhibitors that have been investigated with promising results. Small-molecule PSMA inhibitors bind to the external component of PSMA on the cell surface and are internalized after binding [31]. A recent clinical study using Ga-68-PSMA (Glu-NH-CO-NH-Lys-(Ahx)-[68Ga(HBED-CC)]), for the detection of prostate cancer recurrence in 248 patients with biochemical recurrence after radical prostatectomy demonstrated high detection rates even at relatively low PSA levels [41••]. Detection rates for PSA≥2 ng/mL was 97 %, for PSA 1 to <2 ng/mL was 93 %, for PSA 0.5 to <1 ng/mL was 73 %, and for PSA<0.5 ng/mL was 58 %. The reported detection rate for this Ga-68 PSMA agent is superior to detection rates for C-11 and F-18 choline which are reported to be about 40–60 % for a PSA level below 3 ng/ mL [41••].

Ga-68-labeled PSMA inhibitors have been appealing not only due to increased detection rates but also due to their theranostic counterpart, Lu-177. Ga-68 and Lu-177 are interchangeable theranostic radioisotopes. By exchanging Ga-68 radioisotope with Lu-177, a beta-emitting radioisotope, an imaging agent can be turned into a radiotherapy agent. PSMA-617, a small-molecule PSMA inhibitor which targets the external moiety of PSMA, has been studied with Ga-68-labeling for PET/CT imaging followed by Lu-177 labeling for radiotherapy [42].

F-18-labeled PSMA inhibitors, such as 18F-DCFBC, are also being developed for the evaluation of primary and metastatic disease [43] (Fig. 2). In a recent prospective study of 13 patients, 18F-DCFBC PET demonstrated higher specificity for high-grade (Gleason scores 8 and 9) and larger tumors compared to MRI [44••]. F-18-labeled agents have the advantage of a longer half-life (110 min) compared to Ga-68 halflife (68 min). This allows for centralized production and delivery in a geographic region, akin to the production and delivery of F-18 FDG, which could potentially result in increased commercial availability and distribution of the imaging agent.

FACBC

Anti-1-amino-3–18F-fluorocyclobutane-1-carboxylic acid (FACBC) is an L-leucine amino acid analog which was initially developed for imaging of glioblastomas [35]. FACBC demonstrates increased in vitro uptake in prostate cancer cells and increased in vivo uptake in xenograft nude mouse models likely via the alanine-serine-cysteine amino acid transporter found to be overexpressed in prostate cancer cells [45, 46]. Once it is taken up by the cell, this radiolabeled amino acid analog does not get incorporated into protein synthesis [46]. There is little urinary excretion of FACBC compared to other F-18 PET agents like F-18 FDG and F-18 fluorocholine which makes it a favorable agent for the detection of primary prostate cancer, local recurrence, and metastatic pelvic lymph nodes [34, 45].

Although an initial study with an orthotopic prostate cancer model in rats demonstrated higher FACBC uptake in prostate cancer than in inflammation or benign prostatic hyperplasia [47], in human studies, false-positive uptake in infection, inflammation, benign prostate hyperplasia, and in metabolically active benign bone lesions have been demonstrated [48]. In a prospective study of 21 patients before prostatectomy and hormonal therapy, higher FACBC uptake in tumor compared to normal tissue was demonstrated, but there was overlapping FACBC uptake in cancer, benign prostatic hyperplasia nodules, and prostatic intraepithelial neoplasia resulting in false-positive findings which could be decreased by combining FACBC with MRI [49]. Recent meta-analysis of FACBC for prostate cancer detection demonstrated a pooled sensitivity of 87 % and pooled specificity of 66 % [50].

A prospective study comparing FACBC to ProstaScint® demonstrated better performance of FACBC for the detection of local recurrence and metastatic disease. For local recurrence, FACBC demonstrated 90 % sensitivity, 40 % specificity, 74 % accuracy, and 75 % positive predictive value versus ProstaScint® which demonstrated 67 % sensitivity, 57 % specificity, 64 % accuracy, and 76 % positive predictive value. For metastatic disease, FACBC demonstrated 55 % sensitivity, 97 % specificity, 73 % accuracy, and 96 % positive predictive value versus ProstaScint®, which demonstrated 10 % sensitivity, 87 % specificity, 43 % accuracy, and 50 % positive predictive value [51••].

C-11 Acetate

Acetate is taken up by the cell for the synthesis of fatty acids via fatty acid synthase which is upregulated in prostate cancer [33]. F-18 FDG has proven insensitive for imaging prostate cancer compared to C-11 acetate because fatty acid metabolism rather than glycolysis may

be more important in prostate cancer as demonstrated by the upregulation of fatty acid synthase and by the alteration of many enzymes involved in fatty acid metabolism found in prostate cancer cells [52–54]. C-11 acetate is excreted by the respiratory system with very little urinary excretion [55, 56] which would be advantageous similar to FACBC [57].

Unfortunately, there is considerable overlap of radiotracer uptake in prostate cancer, benign hyperplasia, and normal prostate gland [58]. Meta-analysis for primary prostate cancer detection found a pooled sensitivity of 93 % and specificity of 60 %, but when evaluated on a lesion basis, the pooled sensitivity was 75 % and specificity was 76 % [56]. Although the diagnosis of primary disease may be suboptimal, C-11 acetate may play a role in the detection of lymph node metastases at initial diagnosis. A prospective study of 107 patients with intermediate and high risk localized prostate cancer prior to radical prostatectomy demonstrated that C-11 acetate imaging may detect local metastatic lymph nodes and correlate with treatment-free survival [59]. For detection of recurrence, C-11 acetate performed better for distant metastases and lymph node recurrence with a pooled sensitivity of 82 versus 64 % for local recurrence in the prostate bed, but subanalysis demonstrated 20 % higher sensitivity in prostatectomy patients than in post-radiation patients [56]. Elevated PSA level strongly correlated with sensitivity of C-11 acetate for the detection of recurrent prostate cancer with 35 % lower sensitivity when PSA was less than 1 ng/dL [56].

A disadvantage of C-11 acetate is its short 20-min half-life. This limits its use in routine clinical practice due to the need for an on-site cyclotron. As a result, F-18 acetate with a more favorable radioisotope half-life of 110 min has been studied. Currently, there are no studies comparing the use of C-11 acetate versus F-18 acetate in humans, but a study in monkeys and a pig demonstrated unfavorable blood pool activity, extensive urinary and bile excretion, and defluorination resulting in increased uptake within the skeleton. The study concluded that F-18 acetate was not a useful analog to C-11 acetate [60].

F-18 FDHT

16β−18F-fluoro-5α-dihydrotestosterone (F-18 FDHT) is a radiolabeled 5 α-dihydrotestosterone analog. 5 α-dihydrotestosterone is the main androgen receptor ligand [61]. Androgen receptor (AR) is important in the development and progression of prostate cancer. First-line treatment for systemic treatment of advanced prostate cancer is androgen deprivation therapy (ADT) with surgical or chemical castration which is based on the idea that majority of prostate cancer cells require androgen and the deprivation of androgen will cause prostate cancer cells to die or cease dividing [62]. Although patients with advanced prostate cancer initially respond to ADT, patients often progress to CRPC around 1 to 3 years after starting ADT therapy [63].

The exact mechanism underlying the transition from castration-sensitive to CRPC is unknown, but CRPC is known to have AR alterations that enable the receptor to signal even in the absence of androgen [64]. Even in CRPC, the AR continues to function, plays a role in disease progression, and maintains high expression in most cases of CRPC [65–67]. As a result, there is growing interest in molecularly directed prostate cancer therapies against alterations of the AR [61].

F-18 FDHT binds to the AR and could potentially be used to assess the AR status of prostate cancer for initial treatment planning or for the assessment of treatment efficacy [61]. A feasibility study examining F-18 FDHT for the imaging of AR in 19 patients with advanced prostate cancer demonstrated that the administration of an antiandrogen, flutamide, resulted in decreased FDHT uptake from baseline, and three of five patients who had never received antiandrogen therapy demonstrated no FDHT uptake, suggesting that FDHT could be used to evaluate AR receptor status for initial treatment planning and to monitor results from therapy [32, 62].

Currently, hormonal therapy for breast cancer is determined by estrogen receptor status in biopsy specimens. However, due to potential tumor heterogeneity, evaluation of biopsy sampling could result in sampling bias. Using an in vivo, non-invasive imaging method for the detection of AR could overcome such sampling bias and be an important tool prior to initiating hormonal therapy for prostate cancer with ADT [62]. Given the lower sensitivity for prostate cancer detection compared to FDG (FDHT of 78 and 86 % versus FDG of 97 %), FDHT may be a better imaging agent for in vivo determination of the AR status prior to hormonal therapy and for assessing AR response to therapy than for the detection of prostate cancer [62, 68].

Bombesin/Gastrin-releasing Peptide

Gastrin-releasing peptide (GRP) is a 10-amino acid neuropeptide with many physiological functions in the body and is a mammalian counterpart to bombesin, a neuropeptide initially discovered in the skin of European frogs, *Bombina bombina* and *Bombina variegata* [69]. Mammalian bombesin was identified from pig stomach and found to be a peptide involved in the release of gastrin and hence the name GRP [70]. Since the cloning and characterization of the human GRP, GRP has been found to stimulate tumor growth in several cancers by binding to G-protein-coupled GRP receptors (GRP-R) [71, 72].

There is low expression of GRP-R in normal prostate compared to 45–100 % increased expression in prostate cancers [73]. In vitro studies in prostate cancer cell lines and in vivo studies of xenografts in nude mice have demonstrated that GRP enhanced tumor growth which could be blocked with GRP-R antagonists [72]. GRP/bombesin may also have a role in the development of CRPC. Studies have found overexpression of GRP-R in CRPC [73], and GRP/bombesin has been found to activate the AR and cause the growth of an androgendependent cell line under androgen deprivation conditions [74].

GRP/bombesin analogs binding to GRP-R have been radiolabeled with a variety of radioisotopes including Tc99m and In-111 for gamma camera imaging, with F-18, Cu-64 and Ga-68 for PET imaging, and with Lu-177 and Y-90 for radiotherapy [75–77]. F-18 and Ga-68 labeled GRP/bombesin analogs are both good candidates for PET imaging; however, Ga-68 with its favorable half-life, generator rather than cyclotron production, and theranostic pairing with Lu-177 has garnered much attention.

The first human study with a Ga-68-labeled GRP/ bombesin analog, BAY86–7548, in 14 patients with initial diagnosis of prostate cancer ($n = 11$) or with biochemical recurrence of prostate cancer after prostatectomy or hormonal therapy ($n = 3$) demonstrated 88 %

sensitivity, 81 % specificity, and 83 % accuracy for the detection of primary carcinoma and 70 % sensitivity for the detection of metastatic lymph nodes [76]. The first human study with F-18-labeled GRP/bombesin analog, BAY 864367, in 10 patients with an initial diagnosis of prostate cancer ($n = 5$) or biochemical recurrence ($n = 5$) demonstrated feasibility with higher detection rates in patients with primary prostate cancer than in patients with recurrent disease [78••]. The detection rate was also lower than that for the Ga-68 BAY86–7548 study which could be due to a slight structural difference between the two agents and the variation in Gleason score between the patient populations [78••]. Given the overexpression of GRP/GRP-R detected in the in vitro and in vivo studies in cell lines of several cancers, more human studies using GRP/bombesin analogs for diagnosis and radiotherapy are expected.

Conclusion and Future Directions

Imaging of prostate cancer continues to advance. Current MRI techniques have improved with new developments in diffusion imaging. Many practices have already adopted MRI fusion biopsy and high *b*-value DWI. Novel methods of image processing that extract more information from acquired data are being investigated. Completely novel techniques, such as hyperpolarized MRI, are also in advanced stages of development. A phase 1 study of hyperpolarized substrate MRI for prostate cancer has been completed, and successful larger clinical trials demonstrating effectiveness and improvement in outcomes will need to be performed before this technology enters clinical practice [30]. With regards to PET, new advances in radiopharmaceutical development continue to improve the detection and monitoring of recurrent/metastatic disease. Although these novel PET imaging agents are currently not available for routine clinical use, there are several phase 0 to phase 2 trials investigating the use of these novel PET imaging agents. These investigations include phase 2 clinical trials with FACBC for the detection of recurrent prostate cancer and for guiding radiotherapy in post prostatectomy patients and phase 1 and 2 clinical trials with PSMA agent, 18FDCFBC, for the detection of metastatic prostate cancer [79–81]. There are also phase 0 and phase 1 clinical trials being conducted for Ga-68-labeled bombesin, F-18 FDHT, and Ga-68 PSMA radiopharmaceuticals [82–85]. Future developments in radiopharmaceuticals will also incorporate new PET/MRI scanners which will synergistically combine PET and MRI, likely resulting in improved ability to detect and characterize local disease as well.

References

1•. Crawford ED, Stone NN, Yu EY, Koo PJ, Freedland SJ, Slovin SF, et al. Challenges and recommendations for early identification of metastatic disease in prostate cancer. Urology 2014;83(3):664–9. [PubMed: 24411213] This article reviews the current guidelines for imaging of prostate cancer and provides recommendations that promote early detection of metastatic disease.

2. Poon PY, McCallum RW, Henkelman MM, Bronskill MJ, Sutcliffe SB, Jewett MA, et al. Magnetic resonance imaging of the prostate. Radiology 1985;154(1):143–9. [PubMed: 2578070]

3. Tempany CM, Zhou X, Zerhouni EA, Rifkin MD, Quint LE, Piccoli CW, et al. Staging of prostate cancer: results of Radiology Diagnostic Oncology Group project comparison of three MR imaging techniques. Radiology 1994;192(1):47–54. [PubMed: 8208963]

4. Weinreb JC, Blume JD, Coakley FV, Wheeler TM, Cormack JB, Sotto CK, et al. Prostate cancer: sextant localization at MR imaging and MR spectroscopic imaging before prostatectomy—reults of ACRIN prospective multi-institutional clinicopathologic study. Radiology 2009;251(1):122–33. [PubMed: 19332850]

5. Barentsz JO, Richenberg J, Clements R, Choyke P, Verma S, Villeirs G, et al. ESUR prostate MR guidelines 2012. Eur Radiol 2012;22(4):746–57. [PubMed: 22322308]

6••. American College of Radiology (ACR). PI-RADS: prostate imaging and reporting and data system 2015 version 2 http://www.acr.org/Quality-Safety/Resources/PIRADS/. (Accessed on August 24, 2015).Aims to promote global standardization of mpMRI with regards to acquisition, interpretation, and reporting.

7•. de Rooij M, Hamoen EH, Fütterer JJ, Barentsz JO, Rovers MM. Accuracy of multiparametric MRI for prostate cancer detection: a meta-analysis. AJR Am J Roentgenol 2014;202(2):343–51. [PubMed: 24450675] Metaanalysis demonstrating the accuracy of mpMRI which includes DWI and DCE-MRI.

8. Halpern EJ, Strup SE. Using gray-scale and color and power Doppler sonography to detect prostatic cancer. AJR Am J Roentgenol 2000;174(3):623–7. [PubMed: 10701599]

9. Dimmen M, Vlatkovic L, Hole KH, Nesland JM, Brennhovd B, Axcrona K. Transperineal prostate biopsy detects significant cancer in patients with elevated prostate-specific antigen (PSA) levels and previous negative transrectal biopsies. BJU Int 2012;110(2 Pt 2): E69–75. [PubMed: 22093091]

10. Krughoff K, Eid K, Phillips J, Stoimenova D, Smith D, O'Donnell C, et al. The accuracy of prostate cancer localization diagnosed on transrectal ultrasound-guided biopsy compared to 3-dimensional transperineal approach. Adv Urol 2013;2013:249080. [PubMed: 24470798]

11. Penzkofer T, Tuncali K, Fedorov A, Song SE, Tokuda J, Fennessy FM, et al. Transperineal in-bore 3T MR imaging-guided prostate biopsy: a prospective clinical observation study. Radiology 2015;274(1):170–80. [PubMed: 25222067]

12. Cerantola Y, Haberer E, Torres J, Alameldin M, Aronson S, Levental M, et al. Accuracy of cognitive MRI-targeted biopsy in hitting prostate cancer-positive regions of interest. World J Urol 2015 5 17.

13. Moore CM, Robertson NL, Arsanious N, Middleton T, Villers A, Klotz L, et al. Image-guided prostate biopsy using magnetic resonance imaging-derived targets: a systematic review. Eur Urol 2013;63(1):125–40. [PubMed: 22743165]

14. Cool DW, Zhang X, Romagnoli C, Izawa JI, Romano WM, Fenster A. Evaluation of MRI-TRUS fusion versus cognitive registration accuracy for MRI-targeted, TRUS-guided prostate biopsy. AJR Am J Roentgenol 2015;204(1):83–91. [PubMed: 25539241]

15. Pinto PA, Chung PH, Rastinehead AR, Baccala AA, Kruecker J, Benjamin CJ, et al. Magnetic resonance imaging/ultrasound fusion guided prostate biopsy improves cancer detection following transrectal ultrasound biopsy and correlates with multiparametric magnetic resonance imaging. J Urol 2011;186(4):1281–5. [PubMed: 21849184]

16. Bjurlin MA, Meng X, Le Nobin J, Wysock JS, Lepor H, Rosenkrantz AB, et al. Optimization of prostate biopsy: the role of magnetic resonance imaging targeted biopsy in detection, localization and risk assessment. J Urol 2014;192(3):648–58. [PubMed: 24769030]

17••. Mozer P, Roupret M, Le Cossec C, Granger B, Comperat E, de Gorski A, et al. First round of targeted biopsies using magnetic resonance imaging/ultrasonography fusion compared with conventional transrectal ultasonography-guided biopsies for the diagnosis of localised prostate cancer. BJU Int 2015;115(7):50.Prospective study in 152 men which demonstrated that fusion targeted biopsies detected more clinically significant lesions compared to standard biopsies.

18. Peltier A, Aoun F, Lemort M, Kwizera F, Paesmans M, Van Velthoven R. MRI-targeted biopsies versus systematic transrectal ultasound guided biopsies for the diagnosis of localized prostate cancer in biopsy naïve men. Biomed Res Int 2015:571708. [PubMed: 25692142]

19. Radtke JP, Kuru TH, Boxler S, Alt CD, Popeneciu IV, Huettenbrink C, et al. Comparative analysis of transperineal template saturation prostate biopsy versus magnetic resonance imaging targeted biopsy with magnetic resonance imaging-ultrasound fusion guidance. J Urol 2015;193(1):87–94. [PubMed: 25079939]

20. Schoots IG, Roobol MJ, Nieboer D, Bangma CH, Steyerberg EW, Hunink MG. Magnetic resonance imaging-targeted biopsy may enhance the diagnostic accuracy of significant prostate cancer detection compared to standard transrectal ultrasound-guided biopsy: a systematic review and meta-analysis. Eur Urol 2015;68(3):438–50. [PubMed: 25480312]

21••. Siddiqui MM, Rais-Bahrami S, Turkbey B, George AK, Rothwax J, Shakir N, et al. Comparison of MR/ultrasound fusion-guided biopsy with ultrasound-guided biopsy for the diagnosis of prostate cancer. JAMA 2015;313(4):390–7. [PubMed: 25626035] Large prospective cohort study demonstrating increased detection of high risk lesion and decreased detection of low risk lesions when using targeted MR/ US fusion biopsy.

22. Grant KB, Agarwal HK, Shih JH, Bernardo M, Pang Y, Daar D, et al. Comparison of calculated and acquired high b value diffusionweighted imaging in prostate cancer. Abdom Imaging 2015;40(3): 578–86. [PubMed: 25223523]

23. Katahira K, Takahara T, Kwee TC, Oda S, Suzuki Y, Morishita S, et al. Ultra-high-b-value diffusion-weighted MR imaging for the detection of prostate cancer: evaluation in 201 cases with histopathological correlation. Eur Radiol 2011;21(1):188–96. [PubMed: 20640899]

24. Rosenkrantz AB, Padhani AR, Chenevert TL, Koh DM, De Keyzer F, Taouli B, et al. Body diffusion kurtosis imaging: basic principles, applications, and considerations for clinical practice. J Magn Reson Imaging 2015 6 26.

25. Tamura C, Shinmoto H, Soga S, Okamura T, Sato H, Okuaki T, et al. Diffusion kurtosis imaging study of prostate cancer: preliminary findings. J Magn Reson Imaging 2014;40(3):723–9. [PubMed: 24924835]

26. Viswanath SE, Bloch NB, Chappelow JC, Toth R, Rofsky NM, Genega EM, et al. Central gland and peripheral zone prostate tumors have significantly different quantitative imaging signatures on 3 Tesla endorectal, in vivo T2-weighted MR imagery. J Magn Reson Imaging 2012;36(1):213–24. [PubMed: 22337003]

27. Rezaeilouyeh H, Mahoor MH, Zhang JJ, LaRosa FG, Chang S, Werahera PN. Diagnosis of prostatic carcinoma on multiparametric magnetic resonance imaging using shearlet transform. Conf Proc IEEE Eng Med Biol Soc 2014;2014:6442–5. [PubMed: 25571471]

28. Kwak JT, Xu S, Wood BJ, Turkbey B, Choyke PL, Pinto PA, et al. Automated prostate cancer detection using T2-weighted and high b-value diffusion-weighted magnetic resonance imaging. Med Phys 2015;42(5):2369–78.

29. Wilson DM, Kurjanewicz J. Hyperpolarized 13C MR for molecular imaging of prostate cancer. J Nucl Med 2014;55(10):1567–72. [PubMed: 25168625]

30. Nelson SJ, Kurhanewicz J, Vigneron DB, Larson PEZ, Harzstark AL, Ferrone M, et al. Metabolic imaging of patients with prostate cancer using hyperpolarized [1–13C] pyruvate. Science Translational Medicine 2013 8;5(198):198ra108.

31. Ghosh A, Heston WD. Tumor target prostate specific membrane antigen (PSMA) and its regulation in prostate cancer. J Cell Biochem 2004;91(3):528–39. [PubMed: 14755683]

32. Zaheer A, Cho SY, Pomper MG. New agents and techniques for imaging prostate cancer. J Nucl Med 2009;50(9):1387–90. [PubMed: 19690043]

33. Jadvar H Molecular imaging of prostate cancer with PET. J Nucl Med 2013;54(10):1685–8. [PubMed: 24084704]

34. Mease RC, Foss CA, Pomper MG. PET imaging in prostate cancer: focus on prostate-specific membrane antigen. Curr Top Med Chem 2013;13(8):951–62. [PubMed: 23590171]

35. Apolo AB, Pandit-Taskar N, Morris MJ. Novel tracers and their development for the imaging of metastatic prostate cancer. J Nucl Med 2008;49(12):2031–41. [PubMed: 18997047]

36. Silver DA, Pellicer I, Fair WR, Heston WD, Cordon-Cardo C. Prostate-specific membrane antigen expression in normal and malignant human tissues. Clin Cancer Res 1997;3(1):81–5. [PubMed: 9815541]

37. Jadvar H Molecular imaging of prostate cancer: PET radiotracers. AJR Am J Roentgenol 2012;199(2):278–91. [PubMed: 22826388]

38. Chatalic KL, Veldhoven-Zweistra J, Bolkestein M, Hoeben S, Koning GA, Boerman OC, et al. A novel 111In-labeled antiprostate-specific membrane antigen nanobody for targeted SPECT/CT imaging prostate cancer. J Nucl Med 2015;56(7): 1094–9. [PubMed: 25977460]

39. Oyen WJ, De Jong IJ. Molecular imaging of prostate cancer: tapping into the opportunities. J Nucl Med 2015;56(2):169–70. [PubMed: 25552669]

40. Osborne JR, Green DA, Spratt DE, Lyashchenko S, Fareedy SB, Robinson BD, et al. A prospective pilot study of (89)Zr-J591/prostate specific membrane antigen positron emission tomography in men with localized prostate cancer undergoing radical prostatectomy. J Urol 2014;191(5):1439–45. [PubMed: 24135437]

41••. Eiber M, Maurer T, Souvatzoglou M, Beer AJ, Ruffani A, Haller B, et al. Evaluation of hybrid 68Ga-PSMA ligand PET/CT in 248 patients with biochemical recurrence after radical prostatectomy. J Nucl Med 2015;56(5):668–74. [PubMed: 25791990] Retrospective study demonstrating detection rates in the biochemical recurrent setting which were superior to other imaging modalities.

42. Benesova M, Schafer M, Bauder-Wust U, Afshar-Oromieh A, Kratochwil C, Mier W, et al. Preclinical evaluation of a tailormade DOTA-conjugated PSMA inhibitor with optimized linker moiety for imaging and endoradiotherapy of prostate cancer. J Nucl Med 2015;56(6):914–20. [PubMed: 25883127]

43. Cho SY, Gage KL, Mease RC, Senthamizhchelvan S, Holt DP, Jeffrey-Kwanisai A, et al. Biodistribution, tumor detection, and radiation dosimetry of 18F-DCFBC, a low-molecular-weight inhibitor of prostate-specific membrane antigen, in patients with metastatic prostate cancer. J Nucl Med 2012;53(12):1883–91. [PubMed: 23203246]

44••. Rowe SP, Gage KL, Faraj SF, Macura KJ, Cornish TC, GonzalezRoibon N, et al. 18F-DCFBC PET/CT for PSMA-based detection and characterization of primary prostate cancer. J Nucl Med 2015;56(7):1003–10. [PubMed: 26069305] Small study using an F18 based PSMA agent demonstrated higher specificity for high grade tumors compared to MRI, but overall lower sensitivity. Future studies combining the PET and MRI may allow for better risk based patient management.

45. Schuster DM, Votaw JR, Nieh PT, Yu W, Nye JA, Master V, et al. Initial experience with the radiotracer anti-1-amino-3–18Ffluorocyclobutane-1-carboxylic acid with PET/CT in prostate carcinoma. J Nucl Med 2007;48(1):56–63. [PubMed: 17204699]

46. Okudaira H, Shikano N, Nishii R, Miyahi T, Toshimoto M, Kobayashi M, et al. Putative transport mechanism and intracellular fate of trans-1-amino-3–18F-fluorocyclobutanecarboxylic acid in human prostate cancer. J Nucl Med 2011;52(5):822–9. [PubMed: 21536930]

47. Oka S, Hattori R, Kurosaki F, Toyama M, Williams LA, Yu W, et al. A preliminary study of anti-1-amino-3–18F-fluorocyclobutyl-1-carboxylic acid for the detection of prostate cancer. J Nucl Med 2007;48(1):46–55. [PubMed: 17204698]

48. Schuster DM, Nanni C, Fanti S, Oka S, Okudaira H, Inoue Y, et al. Anti-1-amino-3–18F-fluorocyclobutane-1-carboxylic acid: physiologic uptake patterns, incidental findings, and variants that may simulate disease. J Nucl Med 2014;55(12):1986–92. [PubMed: 25453047]

49. Turkbey B, Mena E, Shih J, Pinto PA, Merino MJ, Lindenberg ML, et al. Localized prostate cancer detection with 18F FACBC PET/ CT: comparison with MR imaging and histopathologic analysis. Radiology 2014;270(3):849–56. [PubMed: 24475804]

50. Ren J, Yuan L, Wen G, Yang J. The value of anti-1-amino-3–18Ffluorocyclobutane-1-carboxylic acid PET/CT in the diagnosis of recurrent prostate carcinoma: a meta-analysis. Acta Radiol 2015 4 22.

51••. Schuster DM, Nieh PT, Jani AB, Amzat R, Bowman FD, Halkar RK, et al. Anti-3-[(18)F]FACBC positron emission tomographycomputerized tomography and (111)In-capromab pendetide single photon emission computerized tomography-computerized tomography for recurrent prostate carcinoma: results of a prospective clinical trial. J Urol 2014;191(5):1446–53. [PubMed: 24144687] Prospective study demonstrating superior performance of FACBC compared to ProstaScint®. FACBC is currently licensed by Blue Earth Diagnostics with plans to commercialize the agent to detect disease in recurrent prostate cancer setting.

52. Pflug BR, Pecher SM, Brink AW, Nelson JB, Foster BA. Increased fatty acid synthase expression and activity during progression of prostate cancer in the TRAMP model. Prostate 2003;57(3):245–54. [PubMed: 14518031]

53. Liu Y Fatty acid oxidation is a dominant bioenergetic pathway in prostate cancer. Prostate Cancer Prostatic Dis 2006;9(3):230–4. [PubMed: 16683009]

54. Vavere AL, Kridel SJ, Wheeler FB, Lewis JS. 1–11C-acetate as a PET radiopharmaceutical for imaging fatty acid synthase expression in prostate cancer. J Nucl Med 2008;49(2):327–34. [PubMed: 18199615]
55. Seltzer MA, Jahan SA, Sparks R, Stout DB, Satyamurthy N, Dahlbomn M, et al. Radiation dose estimates in humans for (11)C-acetate whole-body PET. J Nucl Med 2004;45(7):1233–6. [PubMed: 15235071]
56. Mohsen B, Giorgio T, Rasoul ZS, Werner L, Ali GR, Reza DK, et al. Application of C-11-acetate positron-emission tomography (PET) imaging in prostate cancer: systematic review and metaanalysis of the literature. BJU Int 2013;112(8):1062–72. [PubMed: 23937453]
57. Jadvar H Prostate cancer: PETwith 18F-FDG, 18For 11C-acetate, and 18For 11C-choline. J Nucl Med 2011;52(1):81–9. [PubMed: 21149473]
58. Kato T, Tsukamoto E, Kuge Y, Takei T, Shiga T, Shinohara N, et al. Accumulation of [11C]acetate in normal prostate and benign prostatic hyperplasia: comparison with prostate cancer. Eur J Nucl Med Mol Imaging 2002;29(11):1492–5. [PubMed: 12397469]
59. Haseebuddin M, Dehdashti F, Siegel BA, Liu J, Roth EBNepple KG, et al. 11C-Acetate PET/CT before radical prostatectomy: nodal staging and treatment failure prediction. J Nucl Med 2013;54(5): 699–706. [PubMed: 23471311]
60. Lindhe O, Sun A, Ulin J, Rahman O, Langstrom B, Sorensen J. [(18)F]Fluoroacetate is not a functional analogue of [(11)C]acetate in normal physiology. Eur J Nucl Med Mol Imaging 2009;36(9): 1453–9. [PubMed: 19387639]
61. Beattie BJ, Smith-Jones PM, Jhanwar YS, Schoder H, Schmidtlein CR, Morris MJ, et al. Pharmacokinetic assessment of the uptake of 16beta-18F-fluoro-5alpha-dihydrotestosterone (FDHT) in prostate tumors as measured by PET. J Nucl Med 2010;51(2):183–92. [PubMed: 20080885]
62. Dehdashti F, Picus J, Michalski JM, Dence CS, Siegel BA, Katzenellenbogen JA, et al. Positron tomographic assessment of androgen receptors in prostatic carcinoma. Eur J Nucl Med Mol Imaging 2005;32(3):344–50. [PubMed: 15726353]
63. Cookson MS, Roth BJ, Dahm P, Engstrom C, Freedland SJ, Hussain M, et al. Castration-resistant prostate cancer: AUA guideline. J Urol 2013;190(2):429–38. [PubMed: 23665272]
64. Chen Y, Sawyers CL, Scher HI. Targeting the androgen receptor pathway in prostate cancer. Curr Opin Pharmacol 2008;8(4):440–8. [PubMed: 18674639]
65. Scher HI, Sawyers CL. Biology of progressive, castration-resistant prostate cancer: directed therapies targeting the androgen-receptor signaling axis. J Clin Oncol 2005;23(32):8253–61. [PubMed: 16278481]
66. Montgomery RB, Mostaghel EA, Vessella R, Hess DL, Kalhorn TF, Higano CS, et al. Maintenance of intratumoral androgens in metastatic prostate cancer: a mechanism for castration-resistant tumor growth. Cancer Res 2008;68(11):4447–54. [PubMed: 18519708]
67. Yuan X, Balk SP. Mechanisms mediating androgen receptor reactivation after castration. Urol Oncol 2009;27(1):36–41. [PubMed: 19111796]
68. Larson SM, Morris M, Gunther I, Beattie B, Humm JL, Akhurst TA, et al. Tumor localization of 16beta-18F-fluoro-5alphadihydrotestosterone versus 18F-FDG in patients with progressive, metastatic prostate cancer. J Nucl Med 2004;45(3):366–73. [PubMed: 15001675]
69. Anastasi A, Erspamer V, Bucci M. Isolation and structure of bombesin and alytesin, 2 analogous active peptides from the skin of the European amphibians Bombina and Alytes. Experientia 1971;27(2):166–7. [PubMed: 5544731]
70. McDonald TJ, Jornvall H, Nilsson G, Vagne M, Ghatei M, Bloom SR, et al. Characterization of a gastrin releasing peptide from porcine non-antral gastric tissue. Biochem Biophys Res Commun 1979;90(1):227–33. [PubMed: 496973]
71. Spindel ER, Chin WW, Price J, Rees LH, Besser GM, Habener JF. Cloning and characterization of cDNAs encoding human gastrinreleasing peptide. Proc Natl Acad Sci U S A 1984;81(18):5699–703. [PubMed: 6207529]
72. Van de Wiele C, Dumont F, van Belle S, Slegers G, Peers SH, Dierckx RA. Is there a role for agonist gastrin-releasing peptide receptor radioligands in tumour imaging? Nucl Med Commun 2001;22(1):5–15. [PubMed: 11233552]

73. Ischia J, Patel O, Bolton D, Shulkes A, Baldwin GS. Expression and function of gastrin-releasing peptide (GRP) in normal and cancerous urological tissues. BJU Int 2014;113 Suppl 2:40–7. [PubMed: 24894852]
74. Kung HJ, Evans CP. Oncogenic activation of androgen receptor. Urol Oncol 2009;27(1):48–52. [PubMed: 19111798]
75. Maina T, Nock B, Mather S. Targeting prostate cancer with radiolabelled bombesins. Cancer Imaging 2006;6:153–7. [PubMed: 17098646]
76. Kahkonen E, Jambor I, Kemppainen J, Lehtio K, Gronroos TJ, Kuisma A, et al. In vivo imaging of prostate cancer using [68Ga]labeled bombesin analog BAY86–7548. Clin Cancer Res 2013;19(19):5434–43. [PubMed: 23935037]
77. Liu Y, Hu X, Liu H, Bu L, Ma X, Cheng K, et al. A comparative study of radiolabeled bombesin analogs for the PET imaging of prostate cancer. J Nucl Med 2013;54(12):2132–8. [PubMed: 24198391]
78••. Sah BR, Burger IA, Schibli R, Friebe M, Dinkelborg L, Graham K, et al. Dosimetry and first clinical evaluation of the new 18Fradiolabeled bombesin analogue BAY 864367 in patients with prostate cancer. J Nucl Med 2015;56(3):372–8. [PubMed: 25678494] First in man trial demonstrated safety, tolerability and favorable dosimetry. This study sets the foundation for future trials investigating the use of the bombesin tracer in prostate cancer.
79. Schuster DM; Emory University. 18F-FACBC PET-CT for the detection and staging of recurrent prostate carcinoma. In: ClinicalTrials.gov [Internet] Bethesda (MD): National Library of Medicine (US). 2000 [cited 2015 Sept 15]. Available from: https://www.clinicaltrials.gov/ct2/show/study/NCT00562315 NLM Identifier: NCT00562315.
80. Emory University. Advanced molecular imaging with anti-3[18F]FACBC PET-CT to improve the selection and outcomes of prostate cancer patients receiving post-prostatectomy radiotherapy. In: ClinicalTrials.gov [Internet] Bethesda (MD): National Library of Medicine (US) 2000 [cited 2015 Sept 15]. Available from: https://www.clinicaltrials.gov/ct2/show/NCT01666808 NLM Identifier: NCT01666808.
81. Sidney Kimmel Comprehensive Cancer Center. Evaluation of 18FDCFBC PSMA-based PET imaging for detection of metastatic prostate cancer. In: ClinicalTrials.gov [Internet] Bethesda (MD): National Library of Medicine (US) 2000 [cited 2015 Sept 15]. Available from: https://www.clinicaltrials.gov/ct2/show/NCT01815515 NLM Identifier: NCT01815515.
82. Piramal Imaging SA. PET/CT imaging for radiation dosimetry, plasma pharmacokinetics, biodistribution, safety and tolerability and diagnostic performance of BAY86–7548 in patients with prostate cancer and healthy volunteers. In: ClinicalTrials.gov [Internet] Bethesda (MD): National Library of Medicine (US) 2000 [cited 2015 Sept 15]. Available from: https://www.clinicaltrials.gov/ct2/show/NCT01205321 NLM Identifier: NCT01205321.
83. Stanford University; National Cancer Institute. 68Ga-DOTABombesin PET/MRI in imaging patients with prostate cancer. In: ClinicalTrials.gov [Internet] Bethesda (MD): National Library of Medicine (US) 2000 [cited 2015 Sept 15]. Available from: https://www.clinicaltrials.gov/ct2/show/NCT02440308 NLM Identifier: NCT02440308.
84. Memorial Sloan Kettering Cancer Center. [18F]-fluoro-2-deoxy-Dglucose and -[18F] dihydro-testosterone PET imaging in patients with progressive prostate cancer. In: ClinicalTrials.gov [Internet] Bethesda (MD): National Library of Medicine (US) 2000[cited 2015 Sept 15]. Available from: https://www.clinicaltrials.gov/ct2/show/NCT00588185 NLM Identifier: NCT00588185.
85. Stanford University; National Cancer Institute. 68Ga-PSMA PET/CT or PET/MRI in evaluating patients with recurrent prostate cancer. In: ClinicalTrials.gov [Internet] Bethesda (MD): National Library of Medicine (US) 2000 [cited 2015 Sept 15]. Available from: https://www.clinicaltrials.gov/ct2/show/NCT02488070 NLM Identifier: NCT02488070.

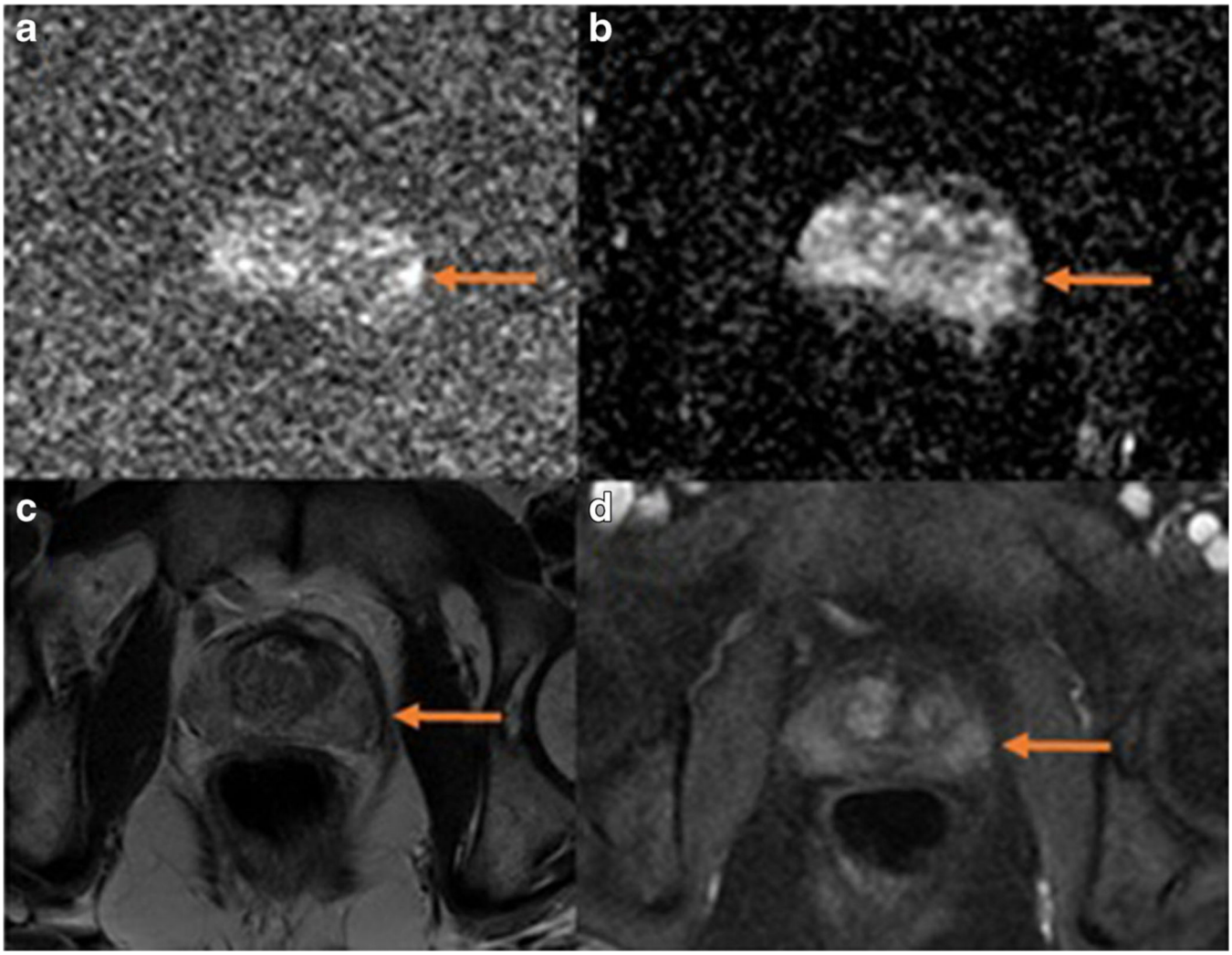

Fig. 1.

A small lesion in the left lateral basal peripheral zone of the prostate gland is seen on mpMRI. The lesion is most conspicuous on DWI as a focus of high signal on high *b*-value images (**a**, *b*=1400) and low signal on ADC map (**b**). It is barely visible above background on T2-weighted images (**c**) and DCE (**d**, early post contrast)

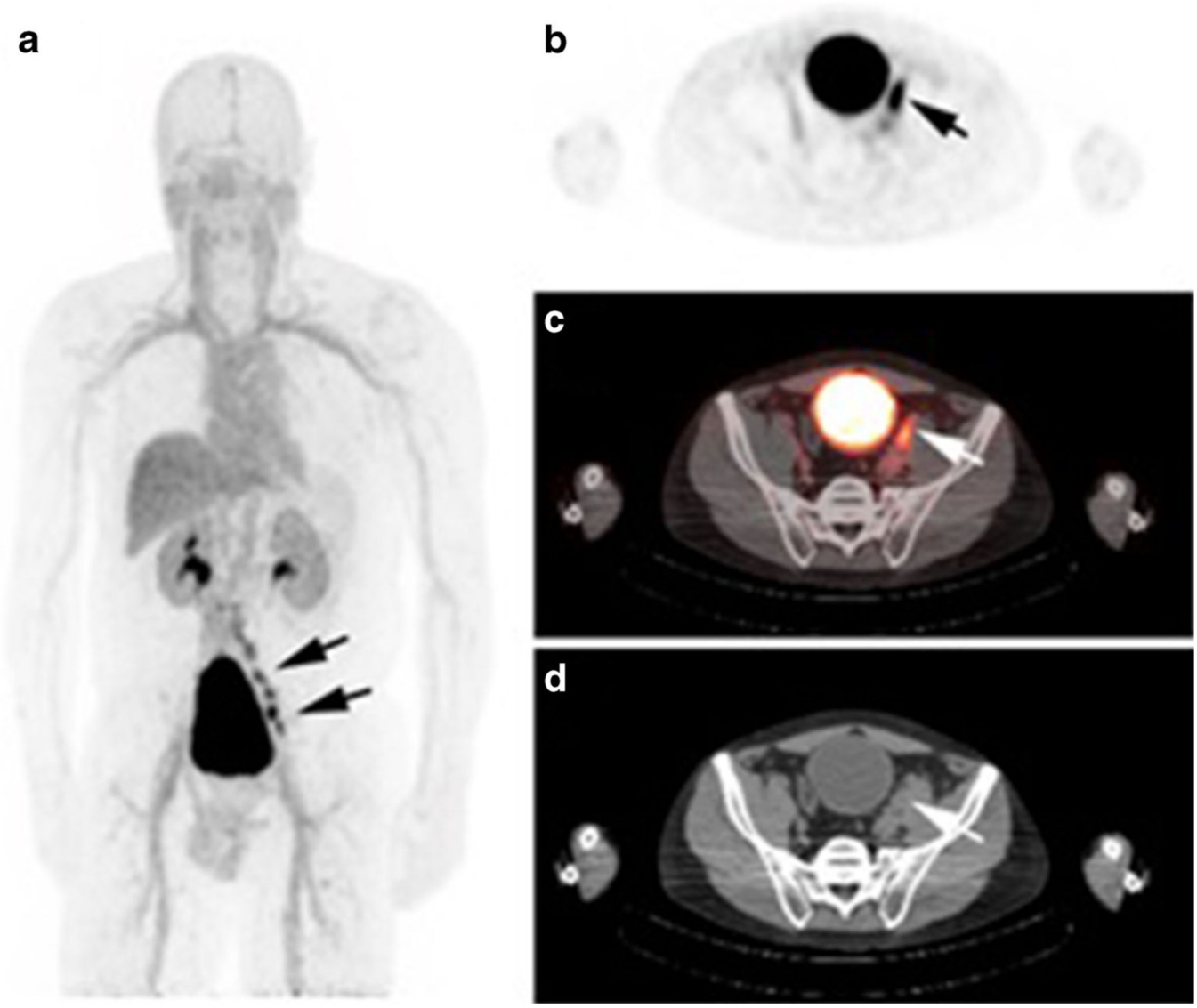

Fig. 2.

A 65-year-old man post prostatectomy presents with biochemical recurrence. PSA at the time of imaging was 1.2 ng/ mL. 18F-DCFBC PET/CT demonstrates multiple positive pelvic nodes on MIP image (**a**). Example of a positive enlarged pelvic node is demonstrated on axial PET image (**b**), fused PET/CT image (**c**), and axial CT image (**d**) [4]